

# High Precision Galvanometer-Based Scanning Lithography System for Nano-scale Machining

Xander Linzel  
xlinzel@uwaterloo.ca

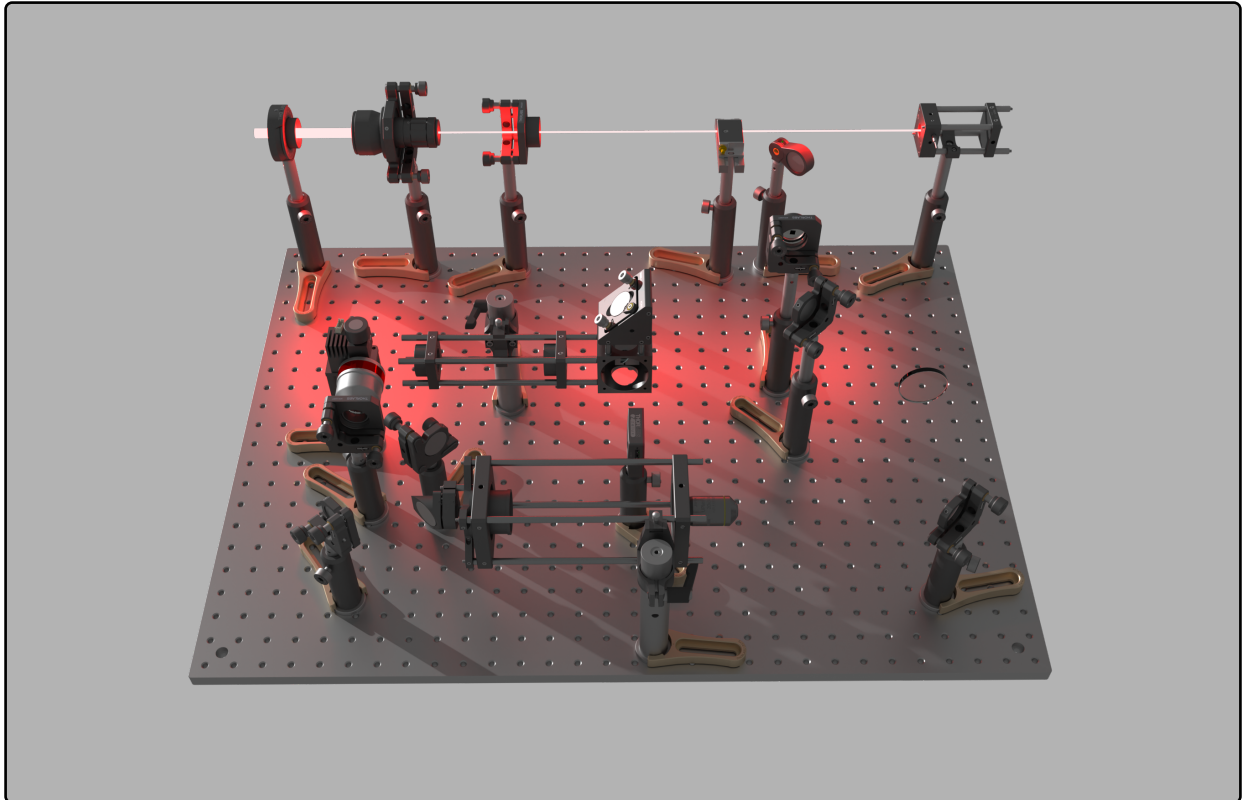


Figure 1: Conceptual overview of the galvanometer-based scanning lithography system.

## 1 PROJECT OVERVIEW AND OBJECTIVES

This system serves as a robust and versatile ultrafast irradiation lithography platform, with the goal of expanding applications and research possibilities for ultrafast high-power laser processing. Such applications require high precision, small feature sizes, fast scan speeds, and a high degree of customization and modularity in order to serve a wide range of research needs. The details of this system are laid out in this document, covering both the overall design and the potential modifications that can be made to suit the needs of the user and alter the performance or cost of the system.

The primary design objectives of the system are as follows. First, to achieve diffraction-limited focusing at 780 nm with effective numerical apertures up to 0.65, yielding spot sizes on the order of 612 nm. Second, to provide a sample-plane field of view approaching  $1 \text{ mm}^2$  through interchangeable objective configurations. Third, to

enable high-speed beam steering with galvanometer step resolution of  $15 \mu\text{rad}$ , translating to sub-50 nm positioning precision at the sample plane. Fourth, to integrate real-time power modulation via an acousto-optic modulator (AOM) and in-situ sample imaging through a CMOS camera path. Finally, the system is intended to achieve these goals at a total cost of approximately \$13,263.76 USD (\$20,983.67 CAD), making it accessible as a research-grade tool without the cost overhead of commercial lithography platforms.

## 2 SYSTEM PERFORMANCE REQUIREMENTS

The fundamental trade-off between feature size and field of view (FOV) can be mitigated by properly understanding the limitations of any given configuration and tailoring the system to the needs of the researcher. The goal of this system is to enable approximately  $1 \text{ mm}^2$  of total patterning area, raw feature sizes between 600–800 nm, and scan speeds capable of at least matching the repetition

rate of the system laser (currently 1 kHz), with sufficient bandwidth overhead to allow for future optimization. In order to achieve these specifications at low cost, a galvanometer-based scanning system was designed with subsystems for automatic power control, sample imaging, and aberration reduction.

## 2.1 Lithographic Resolution and Feature Size Targets

The system was designed to accommodate a range of objectives, allowing the feature size and FOV to be selected for each use case. The raw feature size, determined by the spot size after the focusing objective, ranges from approximately 600 nm to over 1  $\mu\text{m}$  depending on the selected objective, with larger spot sizes providing a correspondingly larger writing FOV. The lithographic resolution of this system is determined by two factors: the signal resolution of the galvanometer controllers and the hard angular movement limits of the galvanometers themselves. The goal is to achieve step resolution well below the feature size, enabling precise positioning for vectorized write paths. By achieving resolution much finer than the spot size, the system may support smooth vectorized scan control, which is more efficient and precise than purely raster-based approaches.

With the selected GVS001 galvanometers (15  $\mu\text{rad}$  mechanical step size) and the 40 $\times$  objective relay configuration, the system achieves a sample-plane step resolution of approximately 40.5 nm. This is well below the diffraction-limited spot size of 612 nm, yielding a step-to-spot-size ratio of approximately 1:15. This satisfies the Nyquist sampling criterion by a wide margin, as confirmed by the system design calculations, and enables smooth vectorized scan trajectories without aliasing or stitching artifacts. The resulting number of step-limited addressable positions across the full field of view is approximately 9,844, compared to roughly 651 spot-size-limited addressable positions, providing ample spatial resolution overhead for complex and high-fidelity patterning tasks.

## 3 SCANNING LITHOGRAPHY SYSTEM ARCHITECTURE

### 3.1 Galvanometer Scan Head Configuration

The beam steering subsystem is built around a pair of Thorlabs GVS001 single-axis galvanometer scanners, arranged in an orthogonal dual-axis configuration to provide full two-dimensional beam deflection. Each galvanometer unit features a 7 mm diameter silver-coated mirror, a maximum mechanical scan angle of  $\pm 20^\circ$  (corresponding to  $\pm 40^\circ$  optical), and a minimum angular step size of 15  $\mu\text{rad}$ . The galvo mirrors are mounted in a GCM001 galvanometer cage mount assembly, which provides precise co-alignment of the two scan axes and integrates directly into the Thorlabs cage system for mechanical stability.

A pair of relay lenses (AC254-060-B-ML,  $f = 60$  mm, 25.4 mm clear aperture, 650–1050 nm AR coating) is positioned in a 4 $f$  configuration between the two galvanometer mirrors. This galvo relay ensures that the pivot point of the first mirror is optically conjugated to the pivot point of the second mirror, minimizing beam walk-off and vignetting that would otherwise arise from the physical separation of the two scan axes. Without this relay, large scan

angles would produce spatial offsets at the scan lens entrance pupil, degrading field uniformity and introducing asymmetric aberrations.

### Core System Components

- *Galvanometer Mirrors and Driver Electronics:* Two Thorlabs GVS001 galvanometers with GPS011-US power supply and GCE001 interconnect cable. Each galvo provides  $\pm 20^\circ$  mechanical scan range with 15  $\mu\text{rad}$  step resolution. The closed-loop servo drivers accept  $\pm 10$  V analog command signals and provide position feedback for calibration and error monitoring.
- *Scan Lens:* A Thorlabs LSM54-850 telecentric  $f$ -theta scan lens with 54 mm focal length, 6 mm clear aperture, and  $\pm 8.4^\circ$  scan angle limit. This lens is optimized for the 750–950 nm wavelength range and provides 17.8 mm maximum scanning distance at its image plane. The  $f$ -theta design ensures that the lateral displacement of the focused spot is linearly proportional to the input scan angle, simplifying pattern generation and calibration.
- *Beam Expansion and Conditioning Optics:* A Thorlabs GBE05-E3 5 $\times$  Galilean beam expander (AR coated for 700–1200 nm) conditions the laser output beam from 2 mm to 10 mm diameter prior to entry into the AOM and scanning subsystem. A WPH10M-780 half-wave plate (25.4 mm aperture, 780 nm design wavelength) mounted in an RSP1 rotation mount provides continuous polarization control for optimizing AOM diffraction efficiency and managing polarization-sensitive interactions at the sample.
- *Laser Source and Power Modulation:* The system is designed for use with an ultrafast laser source at 780 nm wavelength. Active power control is achieved using an AOMO 3200-124 acousto-optic modulator, which provides approximately 70% first-order diffraction efficiency over the 780–850 nm range. The AOM enables rapid intensity modulation synchronized with the scan trajectory, allowing for dose control during patterning. A pair of AC254-200-B-ML relay lenses ( $f = 200$  mm, 25.4 mm aperture, 650–1050 nm AR coating) forms a 4 $f$  system around the AOM, ensuring that the beam waist is centered in the AOM crystal and that the beam profile is preserved through the modulation stage. A TRF90 flip mirror provides a beam pick-off path for power calibration using an external benchtop power meter available in the laboratory.

### Design Considerations

Scan linearity is maintained by the  $f$ -theta characteristics of the LSM54-850, which correct the tangent-function nonlinearity inherent in flat-field scanning. Residual distortion and field curvature at the edges of the scan field can be further compensated through software-based calibration lookup tables derived from reference grid measurements. The galvo bandwidth should be verified against the desired scan speeds to ensure the mechanical response can follow the commanded trajectory without significant lag or overshoot, particularly for high-speed vectorized paths. Thermal stability of the galvo mirrors and relay optics should be considered for long

write sessions, as thermal drift in the mirror coatings or mounting hardware could introduce slow positional errors. The GCM001 cage mount provides a degree of thermal isolation, but active monitoring of the galvo position feedback signal is recommended during extended operations.

### 3.2 Focusing Optics and Objective Compatibility

The scanning beam is relayed from the galvanometer scan head to the sample plane through a tube-lens-objective combination that provides the final demagnification and high-NA focusing. The system uses an Olympus-standard infinity-corrected optical train with a 180 mm tube lens focal length, ensuring compatibility with a wide range of commercially available microscope objectives. The tube lens (Olympus,  $f_t = 180$  mm, 36 mm clear aperture) is positioned appropriately, forming a telecentric relay that maps the scanned beam angle into a lateral position at the objective back aperture.

The angle scan factor of the system is given by the ratio of the scan lens focal length to the tube lens focal length:  $f_{\text{scan}}/f_{\text{tube}} = 54/180 = 0.3$ . Equivalently, the galvo-to-pupil beam expansion factor is  $f_{\text{tube}}/f_{\text{scan}} = 3.33$ , which expands the 2 mm beam at the galvo mirror to approximately 6.67 mm at the objective back aperture.

#### Supported Optical Configurations

- **10× Objective Configuration:** A 10× plan objective ( $f = 18$  mm, NA = 0.25) provides the largest available field of view at 1.6 mm, making it the preferred configuration for coarse patterning, alignment, and rapid survey scans. The spot size in this configuration is  $2.148 \mu\text{m}$ , with a step resolution of 162 nm. The fill ratio at the back aperture is approximately 0.70, meaning the beam significantly underfills the objective pupil; as a result, the effective NA is reduced below the nominal value and the focused spot is larger than the diffraction limit of the full aperture. Despite this, the configuration comfortably satisfies the Nyquist criterion and offers nearly four times the field of view of the 40× configuration, which is advantageous for large-area patterning tasks or for initial sample positioning before switching to a higher-magnification objective.
- **20× Objective Configuration:** The Olympus 20× plan objective ( $f = 9$  mm, NA = 0.40, back aperture = 7.2 mm) provides an intermediate balance between field of view and resolution. The spot size is  $1.07 \mu\text{m}$ , with a step resolution of 81 nm and a sample-plane field of view of 0.7974 mm. With the 6.67 mm beam at the objective pupil, the fill ratio is approximately 0.93, yielding a fill-limited effective NA close to the nominal value. This configuration is well suited to moderate-resolution patterning, process development, and applications where the  $\sim 0.8$  mm FOV is needed to cover larger structures without stitching.
- **40× Objective Configuration:** The Olympus 40× plan objective ( $f = 4.5$  mm, NA = 0.65, back aperture = 5.85 mm) is the primary high-resolution configuration. The fill ratio at the back aperture is approximately 1.14, meaning the beam slightly overfills the pupil. This ensures that the full NA of the objective is utilized, yielding the diffraction-limited spot

size of 612 nm (using  $d = 0.51\lambda/\text{NA}_{\text{eff}}$ ). Overfilling results in some power loss at the aperture edge, but guarantees that the effective NA equals the nominal objective NA of 0.65. The maximum sample field of view is approximately 0.40 mm, limited by the  $\pm 8.4^\circ$  scan angle of the LSM54-850 and the 40× demagnification.

- **Working Distance and Numerical Aperture Considerations:** The working distances of the three objectives are 2.04 mm (10×), 0.65 mm (20×), and 0.56 mm (40×). The 10× provides ample clearance for most substrate and sample holder geometries, while the 20× and 40× impose tighter constraints that require careful consideration of substrate thickness, coverslip presence, and sample mounting height. For applications requiring immersion objectives or very short working distances, the cage-mounted focusing assembly can be adapted with appropriate SM-thread adapters (M41×0.5-to-SM2 adapter, SM2A32, and LCP34 cage plates are included in the BOM for this purpose).
- **Beam Overfill and Back Aperture Matching:** The system design intentionally targets a fill ratio near or above unity for the high-resolution objective. At a fill ratio of 1.14 for the 40× configuration, the Gaussian beam wings are clipped by the back aperture, which slightly reshapes the intensity profile at the focus and produces a marginally larger Airy disk sidelobe relative to an ideally matched beam. However, the benefit of guaranteed full-NA utilization outweighs this minor diffraction penalty for lithographic applications where resolution is paramount. The 20× configuration achieves a fill ratio of approximately 0.93, which is near-optimal and produces only a minor reduction in effective NA relative to the nominal value. The 10× configuration, with a fill ratio of 0.70, underfills the back aperture more substantially; this reduces the effective NA and enlarges the spot size, but avoids any clipping losses and is acceptable given that FOV maximization is the primary goal at this magnification.

#### Design Considerations

Spot size at the sample plane is the primary determinant of minimum feature size and is controlled by the effective NA of the focusing objective. The depth of focus scales as  $\lambda/\text{NA}^2$ , and ranges from approximately  $1.85 \mu\text{m}$  for the 40× configuration to  $12.5 \mu\text{m}$  for the 10×, imposing progressively tighter requirements on sample flatness and focus positioning at higher magnifications. Field curvature introduced by the scan lens and tube lens combination may cause the focal plane to deviate from a flat surface across the scan field; this effect should be characterized during system commissioning and can be partially compensated by modulating the objective  $z$ -position during scanning if a motorized focus stage is added. Alignment tolerances for the tube lens and objective are relatively forgiving due to the telecentric design, but lateral decenteration of the objective relative to the scanned beam axis will introduce coma and should be minimized during assembly.

### 3.3 Galvanometer Motion Control and Data Acquisition

The galvanometer command signals and laser synchronization are managed through a National Instruments NI USB-6002 data acquisition (DAQ) system (\$679 USD). The USB-6002 provides 16-bit analog output resolution, two analog output channels, eight analog input channels, and a maximum output update rate of 5 kS/s.

#### Control Hardware and Capabilities

- *Galvo Positioning Precision and Repeatability:* The GVS001 galvo command interface maps a  $\pm 10$  V analog input to the full mechanical range, with the voltage-to-angle scale factor selectable at 0.5, 0.8, or  $1.0 \text{ V}^\circ^{-1}$ . The galvo's minimum incremental step is  $15 \mu\text{rad}$ . To determine the voltage corresponding to one minimum step:

$$\Delta V_{\text{galvo}} = 15 \mu\text{rad} \times \frac{180^\circ}{\pi \text{ rad}} \times S \quad (1)$$

where  $S$  is the scale factor in  $\text{V}^\circ$ . Evaluating for each setting:

$$S = 0.5 \text{ V}^\circ: \quad \Delta V_{\text{galvo}} = 15 \times 10^{-6} \times 57.296 \times 0.5 = 429.7 \mu\text{V} \quad (2)$$

$$S = 0.8 \text{ V}^\circ: \quad \Delta V_{\text{galvo}} = 15 \times 10^{-6} \times 57.296 \times 0.8 = 687.5 \mu\text{V} \quad (3)$$

$$S = 1.0 \text{ V}^\circ: \quad \Delta V_{\text{galvo}} = 15 \times 10^{-6} \times 57.296 \times 1.0 = 859.4 \mu\text{V} \quad (4)$$

The DAQ least-significant-bit (LSB) voltage over the  $\pm 10$  V output range is:

$$\text{LSB} = \frac{V_{\text{range}}}{2^n} = \frac{20 \text{ V}}{2^n} \quad (5)$$

yielding an LSB of  $305.2 \mu\text{V}$  for the 16-bit USB-6002. The ratio of DAQ LSB to galvo step voltage determines the positioning granularity:

$$\text{Galvo steps per DAQ step} = \frac{\text{LSB}}{\Delta V_{\text{galvo}}} \quad (6)$$

**Table 1: DAQ–galvo resolution matching across scale settings.**

	0.5 V $^\circ$ ( $\pm 20^\circ$ )	0.8 V $^\circ$ ( $\pm 12.5^\circ$ )	1.0 V $^\circ$ ( $\pm 10^\circ$ )
$\Delta V_{\text{galvo}}$ ( $\mu\text{V}$ )	430	688	859
DAQ steps / galvo step	1.41	2.25	2.82

The USB-6002 resolves individual galvo steps at all three scale settings, with the DAQ LSB consistently finer than the galvo minimum step. At the most demanding setting (0.5 V/ $\pm 20^\circ$  range), the USB-6002 still provides 1.4 DAQ LSBs per galvo step, confirming that the 16-bit DAC is not a positioning bottleneck. Higher V/ $^\circ$  settings improve DAQ resolution matching further (up to 2.8 DAQ LSBs per galvo step at 1.0 V/ $^\circ$ ) at the expense of reduced scan range. A 14-bit DAQ (e.g., NI USB-6001) was considered but rejected: at the 0.5 V/ $^\circ$  setting it would skip approximately 2.8 galvo steps per DAQ step, discarding nearly two-thirds of the galvo's mechanical precision and providing inadequate control authority for high-resolution patterning.

- *Closed-Loop Feedback and Calibration:* Each GVS001 galvo provides an analog position feedback signal proportional to the actual mirror angle. This signal can be read by the DAQ analog inputs to implement closed-loop position verification, calibration routines, and drift monitoring. The GPS011-US power supply provides the necessary drive current and feedback conditioning for both galvo axes.
- *NI DAQ-Based Control Architecture:* The intended control scheme will generate the scan trajectory as a sequence of ( $x, y$ ) voltage pairs, streamed to the two DAQ analog output channels at a programmable update rate. A third digital or analog output channel will control the AOM modulation signal for laser blanking and dose control. The DAQ analog inputs can simultaneously acquire the galvo position feedback signals for closed-loop verification.
- *DAQ Upgrade Path:* For maximum scan speed and timing precision, the USB-6002 could be replaced with a higher-end NI DAQ with dedicated analog output hardware (e.g., NI PCIe-6363), which provides hardware-timed waveform generation at update rates exceeding 1 MHz and eliminates software timing jitter entirely.

#### Design Considerations

The timing resolution of the DAQ output determines the maximum achievable scan speed: at a given update rate  $f_{\text{update}}$ , the minimum dwell time per position is  $1/f_{\text{update}}$ . For a 1 kHz laser repetition rate, the update rate must be at least 1 kHz to synchronize one galvo position per laser pulse, but significantly higher rates (tens of kHz or more) are desirable for smooth vectorized trajectories between laser pulses. Synchronization between the scan trajectory and the laser trigger is critical for dose uniformity; jitter in the DAQ output timing or in the software-to-hardware latency can produce positional errors at the sample. Hardware-timed output (available on higher-end NI DAQs) eliminates software timing jitter by clocking the analog output from an onboard oscillator or an external trigger signal.

### 3.4 Pattern Generation and Control Software

Control software for the system has not yet been developed. The intended software stack will run on a standard PC and interface with the NI USB-6002 via the NI-DAQmx driver framework. Key capabilities to be implemented include:

- Pattern import from vector graphics (SVG, DXF) or bitmap images, with conversion to galvo voltage-pair sequences through a calibration transform that accounts for scan lens distortion and objective magnification.
- Support for both raster scan (line-by-line with AOM blanking) and vector scan (contour-following) trajectory modes.
- Laser–galvo synchronization, likely using a clock-triggered scheme where the galvo trajectory is timed to the laser pulse train, with AOM gating for per-pulse dose control.
- Calibration routines using the galvo position feedback signals and reference grid measurements to generate field-distortion correction lookup tables.

## Design Considerations

Key challenges for the software development include managing timing jitter between galvo position and laser pulses, ensuring waveform generation and laser triggering share a common time base over long write sequences, and efficiently streaming large pattern datasets to the DAQ without exceeding memory constraints. These considerations will inform the choice between software-timed and hardware-timed output modes during development.

## 4 POTENTIAL RESEARCH APPLICATIONS AND BACKGROUND

The scanning lithography system described in this document enables a broad range of research activities that benefit from high-resolution, programmable, and rapid laser patterning. Unlike commercial mask-based lithography tools, which are optimized for high-throughput replication of fixed patterns, a galvo-based scanning system provides the flexibility to write arbitrary geometries without masks, change patterns between exposures with zero changeover cost, and integrate tightly with in-situ characterization. The following subsections outline several categories of research applications.

### 4.1 Nano-scale Patterning and Microfabrication

The sub-micrometer spot size and sub-100 nm positioning resolution make this system suitable for direct-write lithography on photoresist-coated substrates, enabling the fabrication of diffractive optical elements, photonic crystal structures, micro-lens arrays, and arbitrary two-dimensional nanostructures. The vectorized scan capability is particularly advantageous for curvilinear geometries (e.g., Fresnel zone plates, spiral phase plates) that are inefficient to produce with raster-only systems. In addition, the system can be applied to surface micro-structuring of metals, polymers, and dielectrics through laser ablation or laser-induced forward transfer (LIFT), where the programmable dose control via the AOM allows fine tuning of the ablation depth or material transfer volume on a per-feature basis. Two-photon polymerization lithography is a natural extension, leveraging the ultrafast pulse characteristics and tight focusing to achieve sub-diffraction-limited feature sizes in photosensitive resins.

### 4.2 Ultrafast Laser-Matter Interaction Studies

Beyond fabrication, the system provides a controlled platform for fundamental studies of ultrafast laser-material interactions. The programmable scan trajectory and dose control allow systematic variation of fluence, pulse count, and spatial overlap on a single substrate, enabling high-throughput parameter sweeps for laser damage threshold measurements, multi-pulse incubation studies, and formation of laser-induced periodic surface structures (LIPSS). The imaging camera provides in-situ feedback, allowing researchers to correlate delivered dose with resulting surface morphology in near-real-time. The use of the 780 nm wavelength is well suited to chromophore-based photochemistry research, including gelatin-silver reduction processes and dye-sensitized polymerization, where the two-photon absorption cross-section at this wavelength can be exploited for volumetric confinement of the photochemical reaction.

## 4.3 Custom and Rapid-Prototyping Research Platforms

A key advantage of the galvo-based architecture over fixed-optic or stage-scanned lithography systems is its inherent flexibility and speed. Pattern changes require only a software update, with no physical reconfiguration of the optical path. This makes the system well suited to rapid prototyping workflows where design iteration speed is critical, such as the development of microfluidic channel layouts, biosensor electrode geometries, or optical waveguide routing. The modular mechanical design (cage system construction, interchangeable objectives, accessible relay optics) also allows the system to be reconfigured for different experimental geometries, including transmission-mode illumination, oblique incidence, or integration with additional diagnostic instruments (spectrometers, fluorescence detectors, etc.) without major redesign.

## 5 SYSTEM COST REDUCTION AND CAPABILITY EXPANSION STRATEGIES

The total estimated system cost is approximately \$13,263.76 USD (\$20,983.67 CAD including tax and currency conversion at  $1.4 \times 1.13$ ). The cost is distributed across optical components, mechanical mounting hardware, and electrical/control subsystems. This section discusses strategies for reducing cost in budget-constrained implementations and for expanding system capability in performance-critical applications.

### 5.1 Cost Reduction Pathways

The most significant cost drivers in the current design are the galvanometer pair (\$2,458), the scan lens (\$1,950), and the beam expander (\$1,034). Two primary strategies are available for reducing system cost in budget-constrained implementations.

First, the AOM and its associated  $4f$  relay optics (\$500 estimated for the modulator, plus two AC254-200-B-ML relay lenses) can be omitted entirely. This removes real-time dose modulation capability, requiring the user to rely on external laser power control (e.g., attenuator or waveplate-polarizer combination) and eliminates per-pulse blanking during scan repositioning. For applications where uniform exposure dose is acceptable and blanking is not critical, this is a straightforward cost saving with minimal impact on patterning resolution.

Second, the  $4f$  galvo relay (two AC254-060-B-ML lenses) can be eliminated by replacing the two independent single-axis galvanometers with a compact dual-axis scan head (e.g., Thorlabs GVS012). A dual-axis head places both mirrors in close proximity on a single mount, reducing beam walk-off to acceptable levels without the need for a relay. This simplifies the optical train and reduces component count, though it constrains future flexibility in mirror spacing and axis alignment.

### 5.2 Capability Expansion Options

For higher performance, several upgrade paths are available. Replacing the  $40\times/0.65$  NA objective with a higher-NA oil-immersion objective (e.g.,  $60\times/1.4$  NA) would reduce the spot size further and enable true sub-diffraction multi-photon lithography, though this

requires immersion oil handling and reduced working distance. Upgrading the galvanometers to resonant scanners would significantly increase scan speed for applications requiring high throughput. Replacing the NI USB-6002 with a PCIe-based multifunction DAQ (e.g., NI PCIe-6363) would provide hardware-timed waveform generation at update rates exceeding 1 MHz, eliminating software timing jitter and enabling much faster scan speeds. Addition of a motorized z-stage would enable focus compensation across the scan field, layer-by-layer 3D printing via two-photon polymerization, and automated focus tracking on non-planar substrates.

### 5.3 Modular System Configuration

The system has been designed around the Thorlabs cage and post system specifically to enable modular reconfiguration. All optical mounts use SM1- or SM2-threaded interfaces with cage-compatible plates and rods, allowing individual subsystems (AOM relay, beam expander, galvo relay, imaging path) to be swapped, rearranged, or removed without disturbing the rest of the optical train. This modularity supports two distinct configuration tiers. A *minimal configuration* omits the AOM and its relay optics, the imaging camera, and the beam expander, retaining only the galvo scan head, scan lens, tube lens, objective, and steering mirrors, at a substantially reduced cost. This is suitable for applications where external power control and alignment are acceptable and where the laser beam diameter is already matched to the galvo aperture. A *full configuration*, as described in the BOM, includes all subsystems and provides the complete set of capabilities (real-time power control, in-situ imaging, polarization control, and calibrated dose delivery). Intermediate configurations can be assembled by selecting subsets of the optional modules based on the specific requirements of the research application.

## 6 EXPECTED CAPABILITIES AND FUTURE DEVELOPMENT

Table 2 summarizes the expected performance of the system in its three supported objective configurations.

**Table 2: Summary of expected system performance.**

Parameter	40× Config.	20× Config.	10× Config.
Objective NA	0.65	0.40	0.25
Fill Ratio	1.14	0.93	0.70
Effective NA	0.65	~0.40	<0.25
Spot size	612 nm	1.07 $\mu$ m	2.148 $\mu$ m
Sample FOV	0.40 mm	0.80 mm	1.6 mm
Step resolution	40.5 nm	81 nm	162 nm
Working distance	0.56 mm	0.65 mm	2.04 mm
Nyquist criterion	OK	OK	OK

The system as designed achieves its primary objectives: sub-micrometer feature sizes, sub-50 nm positioning resolution, and a modular architecture that can be tailored from minimal to full capability. The total cost of the full configuration remains below \$14,000 USD, which is an order of magnitude less than comparable commercial scanning lithography platforms.

Future development priorities include commissioning and calibration of the scan field distortion map, characterization of the galvo dynamic response (bandwidth, settling time, and overshoot) under realistic scan trajectories, development of the control software stack with NI-DAQmx integration, and initial lithographic tests on photoresist-coated substrates. Longer-term goals include integration of a motorized focus stage for 3D patterning and automated focus tracking on non-planar substrates.